

Available online at website: https://journal.bcrec.id/index.php/bcrec

Bulletin of Chemical Reaction Engineering & Catalysis, 20 (2) 2025, 293-306



Original Research Article

Screening Support of Bimetallic Ruthenium-Tin Catalysts for Aqueous Phase Hydrogenolysis of Furfuryl Alcohol to 1,5-Pentanediol

Rodiansono^{1,2*}, Atina Sabila Azzahra¹, Edi Mikrianto^{1,2}, Arif Ridhoni¹, Ikhsan Mustari¹, Anggita Nurfitriani¹, Thea Seventina Desiani Bodoi¹, Rahmat Eko Sanjaya², Eka Suarso³, Pathur Razi Ansyah⁴

¹Catalysis for Sustainable Energy and Environment (CATSuRe), Inorganic Materials and Catalysis (IMCat) Laboratory Lambung Mangkurat University, Indonesia.

²Department of Chemistry, Lambung Mangkurat University, Jl. A. Yani Km 36,0 Banjarbaru 70714, Indonesia. ³Department of Physics Lambung Mangkurat University, Jl. A. Yani Km 36,0 Banjarbaru 70714, Indonesia. ⁴Department of Mechanical Engineering, Lambung Mangkurat University, Jl. A. Yani Km 35,0 Banjarbaru 70714, Indonesia.

Received: 19th February 2025; Revised: 9th April 2025; Accepted: 9th April 2025 Available online: 10th April 2025; Published regularly: August 2025



Abstract

The selective aqueous phase hydrogenolysis of furfuryl alcohol (FFalc) to 1,5-pentanediol (1,5-PeD) using supported bimetallic ruthenium-tin (Ru-Sn) catalysts on various metal oxide supports (e.g., TiO₂, ZnO, ZrO₂, Nb₂O₅, γ -Al₂O₃) and its combination were investigated systematically. The catalysts were prepared via coprecipitation-hydrothermal at 150 °C for 24 h, followed by reduction with H₂ at 400 °C for 2 h. Supported Ru-Sn on TiO₂(A), γ -Al₂O₃, and ZrO₂ catalysts exhibited higher yield of 1,5-PeD (55-69%) than that other catalysts at 180 °C, H₂ 10-30 bar for 3-5 h. However, those supported catalysts showed poor recyclability after the first reaction run, and therefore further examination on γ -Al₂O₃ supported Ru-Sn was performed. The Ru-Sn catalyst supported on γ -Al₂O₃-metal oxide composites (metal oxides: ZrO₂, TiO₂(A), TiO₂(R), ZnO, Nb₂O₅, and C) afforded higher FFalc conversion and yield of 1,5-PeD than that of unmodified γ -Al₂O₃ at 180 °C, H₂ 30 bar for 3 h. Among them, the Ru-Sn/ γ -Al₂O₃-TiO₂(A) (33%) catalyst could afford the highest yield of 1,5-PeD (80%) at 99% conversion FFalc at 180 °C, H₂ 10 bar for 5 h. Around 95% of this catalyst can be recycled after the second reaction run and the activity can be restored to initial after reactivation with H₂ at 400 °C for 2 h with a 69% yield of 1,5-PeD at 97% FFalc conversion.

Copyright © 2025 by Authors, Published by BCREC Publishing Group. This is an open access article under the CC BY-SA License (https://creativecommons.org/licenses/by-sa/4.0).

Keywords: Bimetallic Ru-Sn; aqueous phase hydrogenolysis; furfuryl alcohol; 1,5-pentanediol

How to Cite: Rodiansono, R., Azzahra, A. S., Mikrianto, E., Ridhoni, A., Mustari, I., Nurfitriani, A., Bodoi, T.S.D., Sanjaya, R.E., Suarso, E., Ansyah, P.R. (2025). Screening Support of Bimetallic Ruthenium-Tin Catalysts for Aqueous Phase Hydrogenolysis of Furfuryl Alcohol to 1,5-Pentanediol. Bulletin of Chemical Reaction Engineering & Catalysis, 20 (2), 293-306. (doi: 10.9767/bcrec.20357)

Permalink/DOI: https://doi.org/10.9767/bcrec.20357

1. Introduction

The development of heterogeneous catalysts for the efficient and selective transformation of biomass-derived platform C5-furanic compounds (e.g., furfuraldehyde (FFald), furfuryl alcohol (FFalc), tetrahydrofurfuryl alcohol (THFalc), and 2-methylfuran (2-MeF) into α , ω -diols such as 1,2-,

1,4- or 1,5-pentanediol (PeD) has been attracted great attentions [1,2]. The main approach for the production of 1,2- or 1,5-PeD from C5-furans involved two-steps: (1) hydrogenation of C=O and C=C bonds to THFalc and (2) hydrogenolysis of C-O bond to 1,2-PeD and 1,5-PeD, which the major product of diols was depended on the catalyst properties and reaction conditions (Scheme 1, 1st route) [3–5].

* Corresponding Author.

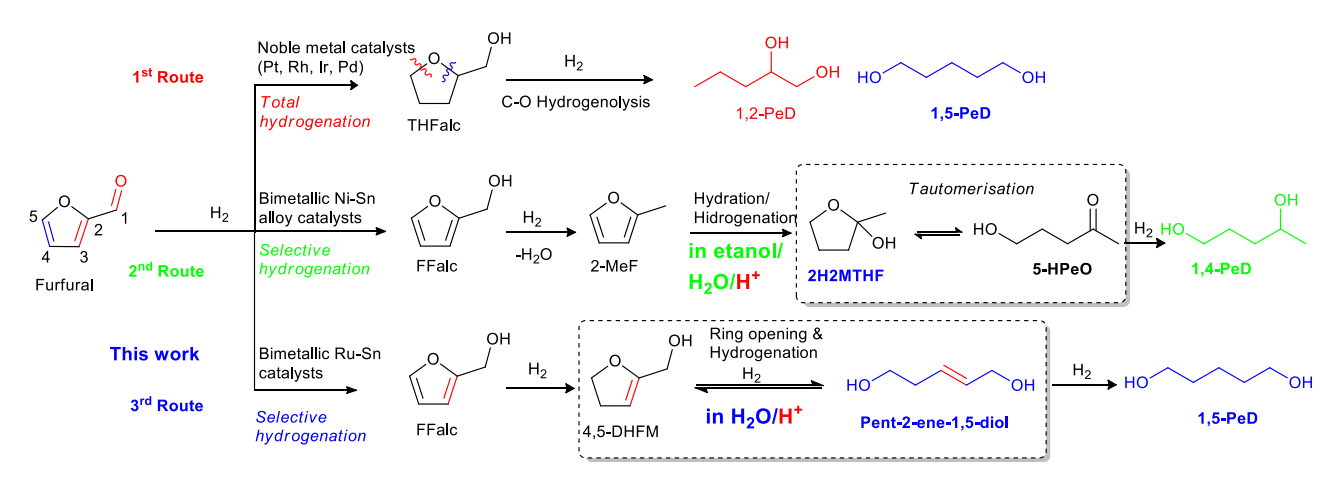
Email: rodiansono@ulm.ac.id (R. Rodiansono)

Catalysts-based on supported platinum metal group (PGM), in the form of monometallic or bimetallic, have been extensively investigated for the synthesis of 1,2-PeD or 1,5-PeD from FFald, THFalc [6–8]. FFalc, or The spinel-type Pt/CoAl₂O₄ catalyst was employed for the direct conversion of FFald to produce 35% 1,5-PeD and 16% 1,2-PeD at 140 °C, and 10 bar H₂ for 24 h [6]. Pt/CeO₂-nanocubes with the ceria-terminal facets exposed (100) afforded higher 1,2-PeD yield (77%) than that of Pt/CeO-nanorods and Pt/CeOoctahedron catalysts [7,8]. Various oxophilic metal oxides-modified Ir-, Rh-, Pd-, Ru-based catalysts demonstrated higher selectivity of 1,5-PeD than those of unmodified counter parts from FFald and its derivatives (e.g., FFalc and THFalc) [9,10]. The oxophilic metal oxides-modified Pd, Ir, Rh, Ni-based catalysts facilitated the C-O bond cleavage of THFalc to produce higher yield of 1,5-PeD than that of 1,2-PeD at high initial H₂ pressure (>80 bar) [11–13]. The layered-double hydroxides of Cu, Co, Al, and Mg-based catalysts were employed for the synthesis of 1,5-PeD from FFald or FFalc [14-17]. The presence of Cu⁰, CoO_x, and basicity of metal oxides synergistically activated the C=C furan ring, followed by the cleavages of C5-O or C2-O bonds to produce 1,2and 1,5-PeD mixtures, respectively [14]. The Cu-Mg₃AlO_{4.5} acted as a bifunctional catalyst for the hydrogenolysis of FFalc, however the mixtures of 1,2-PeD and 1,5-PeD were obtained (80%) [15]. Most recently, the Ni-CoAlO_x system with metallic Ni and CoAlOx [18], hydrotalcite-derived Ni-Co-Al [19], or PtO_x-CoO_x system [20] catalysts with interfacial bimetallic oxides preferentially catalysed the C2-O bond cleavage of furan ring, led to yield of 1,5-PeD higher than that of 1,2-PeD. Most recently, Upare et al. reported that the yield of 1,2-PeD higher than that of 1,5-PeD from FFalc using bimetallic Ru₃Sn₇/ZnO [21] and Ni₃Sn₂/ZnO [22] catalysts due to the combined effect of Ru₃Sn₇ or Ni₃Sn₂ alloy phases together with tin oxide

species on the basicity of ZnO support. Though, several heterogeneous catalysts have been developed, the catalytic reactions inevitably produced the mixture of 1,2-PeD and 1,5-PeD.

Currently, non-precious metal-based on the layered-double hydroxides of Cu, Co, Al, and Mg oxides catalysts have been also developed for the synthesis of 1,5-PeD from FFald or FFalc. The control the basicity and the increase in the density of low-coordination oxygen anions on the support played a prominent role to derive the product selectivity [14-17]. For example, the layered Cu-Co-Al hydrotalcite (LDHs) catalysts served a synergistic action between Cu⁰, CoO_x, and basicity of metal oxides towards partial hydrogenation of C=C furan ring, followed by C2-O bond cleavage to selectively produce 1,5-PeD [14]. The Cu-Mg₃AlO_{4.5} can serve as a bifunctional catalyst for the hydrogenolysis of FFalc to 80% yield of 1,2-PeD and 1,5-PeD mixture [15]. Since there are two competitive reactions pathways: the saturation of C=C bond to THFalc and C-O bond cleavage to 1,2-PeD and 1,5-PeD, the exploration heterogeneous catalyst that allows to the one-step reaction of FFald or FFalc towards high yield 1,5-PeD is greatly challenging. Moreover, in contrast the established approaches above, Dumesic and co-worker proposed the multi-step reactions of FFald; total hydrogenation of FFald to THFalc by using Ni- or Ru-based catalyst, dehydration of THFalc to dihydropyran (DHP) on g-Al₂O₃, hydration-tautomerisation-ring opening of DHP to 5-hydroxy valeraldehyde (5-HY-Val), the finally the hydrogenation of 5-HY-Val to 1,5-PeD on Ru/C catalyst [23]. However, this approach still has drawbacks such as high temperature and initial H₂ pressure and multi-step reaction procedures.

In our group, bimetallic Ni- and Ru-based catalysts have been extensively investigated for the transformation of C5-furan into high-added value of α , ω -diols (1,2-, 1,4- or 1,5-PeD). The presence of second metal Sn in the RANEY®Ni-



Scheme 1. This current work (the 3^{rd} route) on the established routes for the conversion of FFald or FFalc to α, ω -diols using heterogeneous catalysts. 2-MeF = 2-methylfuran; 2H2MTHF = 2-hydroxy-2-methyl tetrahydrofuran; 5-HPeO = 5-hydroxypentanone; 4,5-DHFM = 4,5-dihydrofuranmethanol.

Sn [24,25] or In in RANEY®Ni-In [26] catalysts, in the form of surface-alloyed or intermetallic Ni-Sn or in the presence of Brønsted (Ni-SnO_x) or Lewis acid sites (Ni⁰ or Sn²⁺). They have synergistically played prominent roles in the highly chemoselective hydrogenation of C=O bond in FFald, leading to produce high yield of FFalc and inhibited the C=C bond hydrogenation to THFalc (Scheme 1, 2nd route) ([27–29]. Most recently the gamma-alumina-supported bimetallic ruthenium-tin nanoparticles (Ru- $(x)Sn/\gamma-Al_2O_3$; x = Sn co-loaded) catalysts for the direct conversion of FFald have been developed by Rodiansono et al. [30]. Obviously, a high yield of 1,5-PeD (82%) without the formation of 1,2-PeD and THFalc was achieved over Ru-(1.30)Sn/y-Al₂O₃ at 180 °C, 30 bar H₂, for 3 h and the yield of 1,5-PeD reached up to 94% after a reaction time was extended to 7 h (Scheme 1, 3rd route). this Ru-(1.30)Sn/ γ -Al₂O₃ though exhibited excellent in activity and selectivity for conversion of FFald to 1,5-PeD, one important drawback of recyclability and reusability has remained. It was found that only 90% catalyst weight can be recycled from the reaction mixture after the second reaction and moreover, a notable decrease in FFald conversion and 1,5-PeD yield with quiet amount of remained FFalc product was observed. Therefore, the support screening for Ru-Sn catalyst on various metal oxide supports (e.g., TiO_2 , ZnO, ZrO_2 , Nb_2O_5 , γ - Al_2O_3) and its combination were paid attention. Obviously, the presence of active carbon (C) or TiO2 on the surface of γ-Al₂O₃ could significantly enhance the recyclability of Ru-Sn/C-y-Al₂O₃ [31] and Ru-Sn/y-Al₂O₃-TiO₂ [32] catalysts. Herein, the extended works on the investigation of modified γ-Al₂O₃ supported Ru-Sn(1.30) catalysts for selective direct conversion of FFalc to 1,5-PeD were described systematically. The supported Ru-Sn(1.30)/ γ -Al₂O₃-TiO₂ (33%) catalyst demonstrates a higher yield of 1,5-PeD and recyclability than that of other supported catalysts. The catalytic reaction of FFalc over various supported Ru-Sn catalysts other than of γ -Al₂O₃ in the FFalc conversion to 1,5-PeD was also carried out and discussed.

2. Materials and Methods

2.1 Materials

Ruthenium(III) chloride x hydrate (RuCl₃· xH₂O), furfuryl alcohol (95% GC), dodecane (99%), 2-methoxyethanol, ZrO₂, Nb₂O₅, and ZnO were purchased from Sigma Aldrich Co. The active charcoal (AC) ($S_{BET} = 600 \text{ m}^2.\text{g}^{-1}$) and γ -Al₂O₃ (S_{BET} 129 m².g⁻¹) were purchased from Merck Millipore Co. Sodium hydroxide (NaOH pellet, 99.0%) and ethanol (C₂H₅OH, 96%) purchased from Sigma-Millipore. TiO2 anatase $(TiO_2(A))$ and TiO_2 rutile $(TiO_2(R))$ were purchased and used received as from Hongwunewmaterial (HWNANO) Ltd Co.

2.2 Methods

2.2.1 Catalyst preparation

The preparation of the catalyst has been conducted in a two-stage processes, as illustrated in Figure 1.

Preparation of γ -Al₂O₃-TiO₂(A)

The $\gamma\text{-}Al_2O_3\text{-}TiO_2(A)$ (33%) support was prepared using solid mixing of a 67 wt% $\gamma\text{-}Al_2O_3$

a) Preparation of Al₂O₃-TiO₂(33 wt%)



b) Preparation of Ru-(1.30)Sn/γ-Al₂O₃-TiO₂

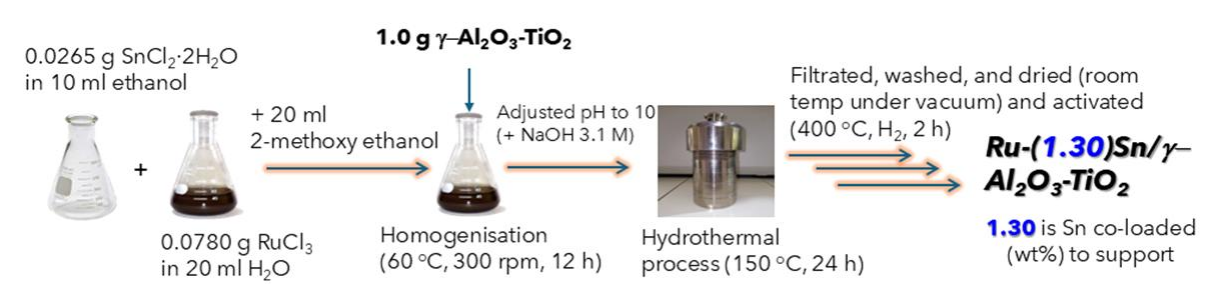


Figure 1. Schematic diagram of the preparation procedure of γ -Al₂O₃-TiO₂(A) and Ru-Sn γ -Al₂O₃-TiO₂(33%) catalyst.

and 33 wt% $TiO_2(A)$ using an oxalic acid as binder at room temperature to form a pasta. The mixture was dried at 110 °C for 12 h, then followed by calcination 300 °C under N_2 for 2 h [32].

Preparation of Ru-Sn/y-Al₂O₃-TiO₂ (33%)

Typical procedure for the synthesis of Ru- $Sn/\gamma - Al_2O_3 - TiO_2(A)(33\%)$ (Ru = 4 wt% and Sn = 1.30 wt%) is described as follows [30,33]. A 0.0768 g (0.3702 mmol) of ruthenium(III) chloride x hydrate (RuCl₃ · xH₂O) was dissolved in deionised water (denoted as solution A) and 0.0245 g (0.1086 mmol) SnCl₂·2H₂O was dissolved in ethanol/2methoxy ethanol (2:1) (denoted as solution B) at room temperature under gentle stirring. A onegram γ -Al₂O₃-TiO₂(A) (33%), solution A, and B were mixed at the room temperature, then the temperature was raised to 50 °C and kept in stirring for 12 h. The pH was adjusted to 9-10 by addition dropwise of an aqueous solution NaOH (3.1 M). The mixture was transferred to the sealed-Teflon autoclave reactor for hydrothermal processes at 150 °C for 24 h. The obtaining black solid precipitate was washed with distilled water and acetone and then dried in vacuo for overnight. Prior to characterisation and catalytic reaction, the black solid of Ru-Sn/y-Al₂O₃-TiO₂(A) (33%) was reduced with hydrogen at 400 °C for 2 h.

2.2.2 Catalyst characterisations

The X-ray diffraction (XRD) analysis was performed on a Miniflex 600 Rigaku instrument with Cu as monochromatic source of Cu-Ka radiation ($\lambda=0.1544$ nm). The XRD was operated at 40 kV and 15 mA with a step width of 0.02°, a scan speed of $4^{\rm o}\, {\rm min^{-1}}\, (\alpha 1=0.1540$ nm, $\alpha 2=0.1544$ nm), solar slit 1.25°, and using a Ni Kß filter. ICP measurements were performed on an SPS 1800H plasma spectrometer by Seiko Instruments Inc. Japan (Ru: 267.87 nm and Sn: 189.898 nm).

The Brunauer-Emmett-Teller (BET) surface area ($S_{\rm BET}$) and pore volume ($V_{\rm p}$) were measured using N₂ physisorption at -196 °C on a Belsorp Max (BEL Japan). The samples were degassed at 200 °C for 2 h to remove physisorbed gases prior to the measurement. The amount of nitrogen adsorbed onto the samples was used to calculate the $S_{\rm BET}$ via the BET equation. The pore volume was estimated to be the liquid volume of nitrogen at a relative pressure of approximately 0.995 according to the Barrett–Joyner–Halenda (BJH) approach based on desorption data [34].

The NH₃-TPD was conducted on a Belsorp Max (BEL Japan). The samples were degassed at elevated temperature of 10-200 °C for 2 h to remove physisorbed gases prior to the measurement. The temperature was then kept at 200 °C for 2 h, while flushed with helium gas. NH₃ gas (balanced NH₃, 80% and He, 20%) was

introduced at 100 °C for 30 min, then evacuated by helium gas to remove the physisorbed NH_3 also for 30 min. Finally, temperature programmed desorption was conducted at temperature of 100-800 °C and the desorbed NH_3 was monitored by TCD.

The H_2 -TPR was performed on a Chemisorb 2750, Micromeritics. The samples were heated at 110 °C for 2 h under N_2 stream with a flow rate of 40 ml/min, then cooled to room temperature. Before reduction processes, the line was purged with H_2 (5% Ar gas v/v) for 30 min, then reduced with the same gas (H_2 (5% Ar v/v)) at elevated temperature of 30-700 °C with ramping 10 °C/min. The H_2 uptake was calculated by using calibration curve (H_2 gas; 5% Ar gas v/v, and flow rate of 40 ml/min).

The calculation of the mean metal particle size (d_{VA}) from H_2 can be achieved based on the volume—area mean diameter equation, Eq. (1) [35]:

$$d_{\text{VA}} = \frac{6v_{\text{m}}}{(Da_{m})} \tag{1}$$

where, D is metal dispersion (the ratio of the total number of metal atoms on the support surface to the total number of metal atoms in the bulk sample), υ_m is the volume occupied by a metal atom (m) in the bulk $(13.65 \times 10^{-3} \text{ nm}^3 \text{ for Ru})[36]$ and $a_{\rm m}$ is the surface area occupied by an exposed surface metal atom (m). The unit cell of hcp Ru has only two atoms and when the (0 0 1) plane is exposed, the surface will have one Ru atom available for H₂ adsorption. When the(1 1 0) plane is exposed, two Ru atoms will be exposed including the atom at the (1/3, 2/3, 1/2) position. In addition, reported results have shown that two other lowindex planes, the (0 0 1) and (1 1 0) planes, have similar levels of surface energy compared to the (1 00) plane of Ru [20]. Therefore, the (100), (001), and (1 1 0) low-index planes may contribute equally to H2 adsorption. So similar to the treatment by Masthan et al. [37] (1 0 0), (0 0 1), and (1 1 0) planes are used to calculate exposed crystal-plane area (am) instead of using only the (1 0 0) plane. Therefore, the surface area occupied by one Ru atom (am) (average from areas of (10 0), (0 0 1), and (1 1 0) planes) is 9.09 x 10⁻² nm² instead of 6.35 x 10-2 nm2 when assuming that only the (0 0 1) plane is exposed.

D (metal dispersion, %) =
$$(V_{\text{mon}}/22414) \times S \times M \times 100/(\text{metal weight}\%)$$
 (2)

where, V_{mon} = monolayer coverage of H_2 on Ru, cm³/g STP, M = atomic mass of metal; 101.07 g/mol, and S = stoichiometric factor of H_2 to Ru atom. H_2 is assumed to be dissociatively adsorbed on Ru metal surfaces, which is S = 2, as most researchers use it [37,38].

2.2.3 Catalytic reactions

Typical catalytic reaction procedure is described as the follows. Catalyst (50 mg), FFalc (2 mmol), dodecane (0.02 mmol), and H₂O (3 mL) as solvent were placed into a glass reaction tube, which fitted inside a stainless-steel reactor. The reactor was flushed with H₂ for ~30 times, after an initial H2 pressure of 10 bar was introduced at room temperature, the reactor was heated to the determined temperature of 140 °C. After 3 h, the reaction mixtures were transferred into sample bin, centrifuged (~5000 rpm for 10 min) and analysed by using GC-FID. The used Ru-Sn/γ-Al₂O₃-TiO₂ (33%) catalyst was separated using either simple centrifugation or filtration, dried overnight under vacuum at temperature, and re-activated with H2 at 400 °C for 2 h prior to reusability testing.

2.2.4 Product analysis

GC analyses of the reactant (FFalc) and products (1,5-PeD, THFalc, 4,5-DHFM) were performed on a Perkin Elmer Auto System XL equipped with a flame ionization detector and Restek Rix® BAC Plus 1 capillary column. GC analysis was operated at detector and injector temperatures of 250 °C and 240 °C, respectively, N₂ as a carrier gas (14 mL/min), rates of air and H₂ were 450 ml/min and H₂ 45 mL/min, respectively. Products were confirmed by the comparison of their GC and GC-MS retention time and mass spectra with the literatures, except for 4,5-DHFM due to the limitation of commercial availability.

The calibration curve was performed using known concentrations of internal standard (ndodecane), reactant and products to determine the correct response factors. The conversion of FFalc and the yield of the products were calculated according to the following equations:

$$Conversion = \frac{F_0 - F_t}{F_0} \times 100\%$$

$$Yield = \frac{mol \ product}{F_0} \times Conversion$$
(4)

$$Yield = \frac{mol \ product}{F_0} \times Conversion \tag{4}$$

where, F_{θ} is the introduced mol reactant (FFalc), F_t is the remained mol reactant, which are all obtained from GC analysis using an internal standard technique.

The apparent reaction rates of the products were calculated using the following equation:

$$r_{1,5-PeD} = \frac{w}{m.t} \times x_{\text{FFalc}} \times x \, s_{\text{Product}}$$
 (5)

where, $r_{1,5\text{-PeD}}$ is the apparent reaction rate of 1,5-PeD (mmol g_{cat}⁻¹ min⁻¹), W is the molar weight of product (mol of product), t is the reaction duration (s), x_{FFalc} is the conversion of FFalc (%), s_{Product} is the selectivity of the product, and *m* is the catalyst weight (g).

3. Results and Discussion

3.1 Catalytic Reaction of Furfuryl Alcohol to 1,5-Pentanediol

3.1.1 Screening of catalyst support

The general reaction scheme for the aqueous phase conversion of FFalc using supported Ru-Sn catalysts is shown in Scheme 2. In attempting to find the most suitable heterogeneous supported ruthenium catalyst for aqueous hydrogenolysis of FFalc to diols (1,2-PeD or 1,5-PeD), the effect of the second metal addition to the supported Ru was investigated. The synthetic procedure of supported bimetallic Ru-Sn catalysts the amount of Sn was set to obtain Ru/Sn molar ratio of 3.0 according to the previous report [33].

Scheme 2. General reaction pathways for the aqueous phase hydrogenolysis of FFalc using supported bimetallic Ru-Sn catalysts.

The results of catalytic reaction of FFalc over various supported bimetallic Ru-Sn are summarised in Table 1.

The $Ru-Sn/TiO_2(R)$ catalyst has poor selectivity towards 1,5-PeD (3%) while the main products were THFalc (55%) and CPO (27%) (entry 1). As expected, Ru-Sn/TiO₂ (A) catalyst afforded 55% 1,5-PeD, 2% 4,5-DHFM, 9% THFalc, 4% CPO at 70% conversion of FFalc (entry 2). The Ru-Sn/Nb₂O₅ showed 100% conversion of FFalc with yields of 1,2-PeD, THFalc, undesired products were 18%, 73%, and 9%, respectively (entry 3). Interestingly, γ -Al₂O₃ and ZrO₂ supported Ru-Sn catalysts afforded high yield of 1,5-PeD (55-69%) at 74-78% conversion of FFalc (entries 4-5) which laterally opposite with their supported monometallic Ru as discussed above (Table 1). In our recently published work, we have described the selective hydrogenolysis of FFald to 1,5-PeD over Ru-(x)Sn/y-Al₂O₃ catalysts in H₂O solvent. We found that the highest yield of 1,5-PeD (82%) was obtained over the most effective Ru-(1.30)Sn/γ-Al₂O₃ at 180 °C, H₂ 30 bar for 3 h, and 94% 1,5-PeD can be reached after reaction for 7 h [30]. Though both γ -Al₂O₃ and ZrO₂ supported Ru-Sn catalysts exhibited higher yield of 1,5-PeD than that of various supported Ru-Sn catalyst, the degree of recyclability and reusability of these catalysts are still the main of drawback. Therefore, the effect of support compositions of bimetallic Ru-Sn on the FFalc conversion, yield of 1,5-PeD, degree of recyclability and reusability are subsequently evaluated. Additionally, the C (charcoal), MgO, and ZnO-supported Ru-Sn catalysts have low activity and selectivity to target product of 1,5-PeD (entries 6-8).

3.1.2 Evaluation of composited-supports

To get insight into the role of support compositions on the FFalc conversion and 1,5-PeD yield, the composites of γ -Al₂O₃-charcoal (C) and

γ-Al₂O₃-metal oxides (e.g., ZrO₂, ZnO, Nb₂O₅, and TiO₂) supported Ru-Sn catalysts were prepared and the reaction results are summarised in Table 2. The utilisation of γ-Al₂O₃ based support for Ru-Sn was due to the fact that both the supported monometallic Ru and bimetallic Ru-Sn on γ-Al₂O₃ catalysts exhibited the highest conversion of FFald as has been described in the recently previous published work [30]. Firstly, Ru-Sn/γ-Al₂O₃-C (charcoal) was evaluated for the reaction and unfortunately, FFalc conversion was only 38% to produce 16% 1,5-PeD, 8% THFalc, and 13% CPO (entry 1), indicating the composited γ-Al₂O₃-C support in the current composition is not suitable for production high yield of 1,5-PeD. Further investigation into this catalyst system was conducted in our research group and the results had been published previously [31]. It was found that the optimised composition of γ-Al₂O₃-C was 70 wt% of C with highest yield of 1,5-PeD (87%), 70% recyclability, and 1,5-PeD yield slightly decreased to 52%. The Ru-Sn/y-Al₂O₃-ZrO₂ (33%) catalyst afforded 52% 1,5-PeD, 13% 4,5-DHFM, 16% CPO, and 12% others (levulinic acid) at 93% conversion of FFalc (entry 2). The quite large amount of CPO (16%) and levulinic acid (12%) indicates that the acidities of γ-Al₂O₃ and ZrO2 may play a key role in the rearrangement of the furan ring in aqueous phase reaction. Li and Deng noticed that the presence of both Brønsted and Lewis acid in the supported metal catalysts functioned as metal-acid tandem catalysis for hydrogenative rearrangement of furfural or furfuryl alcohol into cyclic compounds (e.g. CPO and CPL) or levulinic acid [39]. Interestingly, over Ru-Sn/γ-Al₂O₃-TiO₂(A) (33%) catalyst, a 56% yield of 1,5-PeD was obtained at 81% conversion of FFalc (entry 3). Over this catalyst, the partial hydrogenation of FFalc had also occurred as indicated by the formation of 4,5-DHFM (7%) and others (levulinic acid) (7%) which

Table 1. Results of aqueous phase hydrogenolysis of FFalc using various supported Ru-based catalysts. Reaction conditions: Cat. (0.05 g), FFalc (2.0) mmol, H₂O (3 mL), H₂ (30 bar), 180 °C, 3 h. ^a Conversion and yield were determined by GC (FID) using an internal standard technique. The carbon balance was more than 95% for all the reactions. ^b Unknown condensation product of FFalc (according to the GC-MS data).

	Catalyst	C	Yield ^a (%)						
Entry		Conv. ^a (%)	1,5-PeD (1,2-PeD)	4,5- DHFM	THFalc	CPO (CPL)	2-MeF (2- MeTHF)	Others^b	
1	Ru-Sn/TiO ₂ (R)	95	3	0	55	27	0	10	
2	Ru - Sn/TiO_2 (A)	70	55	2	9	4	0	0	
3	Ru - Sn/Nb_2O_5	100	0(18)	0	73	3	3	3	
4	Ru-Sn/γ–Al ₂ O ₃	74	69	0	5	0	0	0	
5	Ru - Sn/ZrO_2	78	55	0	7	16	0	0	
6	Ru-Sn/C	100	0(18)	0	74	0	4	4	
7	Ru-Sn/ZnO	51	0(2)	0	45	4	0	0	
8	Ru-Sn/MgO	63	0(10)	0	53	0	0	0	

may be competitively occurred with the total hydrogenation of furan ring or rearrangement produced THFalc (5%) or CPO (6%), respectively. The composites of γ-Al₂O₃-TiO₂(R), γ-Al₂O₃-ZnO, and γ-Al₂O₃-Nb₂O₅ supported Ru-Sn catalysts showed low FFalc conversion of 14-43% (entries 4-6) with maximum yield of 1,5-PeD (37%) obtaining over Ru-Sn/ γ -Al₂O₃-TiO₂(R) catalyst (entry 4). Therefore, it can be concluded that the Ru-Sn/γ-Al₂O₃-TiO₂(A) (33%) catalyst the optimised support composition of bimetallic Ru-Sn catalyst system for selective synthesis of 1,5-PeD from FFalc via aqueous phase hydrogenolysis. This catalyst then will be further evaluated the effect of composition of γ-Al₂O₃ to TiO₂(A), reaction parameters (temperature, initial H₂ pressure, time profiles, and recyclability-reusability) on the FFalc conversion and yield of 1,5-PeD.

3.1.3 Catalytic Reaction of FFalc over Ru-Sn/ γ -Al₂O₃-TiO₂(A)

3.1.3.1 Effect of γ -Al₂O₃-TiO₂(A) compositions

In order to establish and to get insight into the Ru-Sn/ γ -Al $_2$ O $_3$ -TiO $_2$ (A) catalyst in aqueous phase hydrogenolysis of FFalc to 1,5-PeD, the different composition of γ -Al $_2$ O $_3$ -TiO $_2$ (A) supports were prepared. The weight percentages of TiO $_2$ (A) to γ -Al $_2$ O $_3$ were designed as 13 wt%, 33 wt%, 67 wt%, and 87 wt% and prepared by physical mixing at room temperature with oxalic acid as a binder, dried at 80-100 °C overnight, followed by calcination at 300 °C under N $_2$ for 2 h, then utilised as the support of Ru-Sn.

Figure 2 shows the results of FFalc reaction using supported Ru-Sn with different support compositions at 180 °C, H_2 30 bar for 3 h. Over Ru-Sn/ γ -Al₂O₃-TiO₂(A) (13%) catalyst, the negative effects of 10 wt% TiO₂(A) addition on the conversion and product distributions were clearly observed. At a 99% FFalc was converted into 42% 1,5-PeD, 3% THFalc, 7% CPO, 17% 4,5-DHFM,

and 30% others. When the amount of TiO₂(A) was increased to 33 wt% to form Ru-Sn/y-Al₂O₃-TiO₂(A) (33%) catalyst, 81% FFalc was converted to produce 1,5-PeD (56%), THFalc (5%), CPO (6%), 4,5-DHFM (7%), and others (dimer of FFalc) (7%). The increase in the TiO₂(A) loading amount to 67 wt% to form Ru-Sn/γ-Al₂O₃-TiO₂(A) (67%) catalyst resulted in the increase in the conversion of FFalc (99%). However, the yield of 1,5-PeD drastically decreased to 37% and the other products were 12% THFalc, 15% CPO, 10% 4,5-DHFM, and 25% others. Further increase of TiO₂(A) to 87 wt% to Ru-Sn/ γ -Al₂O₃-TiO₂(A) (87%)afforded only 14% 1,5-PeD at nearly completed reaction of FFalc. The effects of synthetic parameters (temperature of calcination and reduction) and reaction conditions on the FFalc conversion and yield of 1,5-PeD have been also

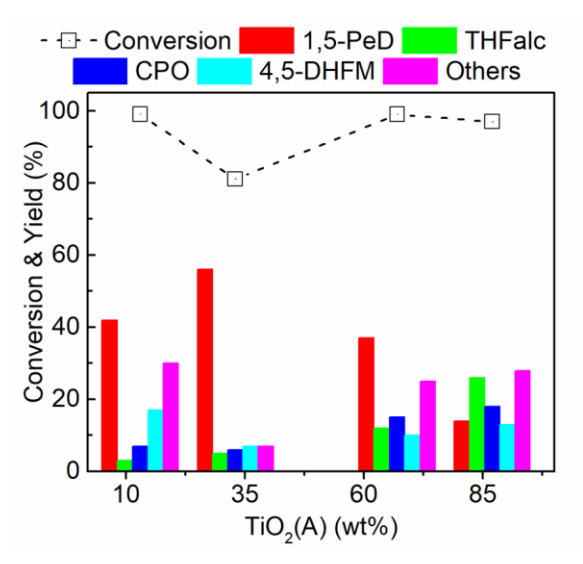


Figure 2. Results of aqueous phase hydrogenolysis of FFalc to 1,5-PeD, the different composition of γ -Al₂O₃-TiO₂(A) supports. Reaction conditions: Cat. (0.05 g), FFalc (2.0) mmol, H₂O (3 mL), H₂ (30 bar), 180 °C, 3 h.

Table 2. Results of aqueous phase hydrogenolysis of furfuryl alcohol using various supported Ru-based catalysts. Reaction conditions: Cat. (0.05 g), FFalc (2.0) mmol, H_2O (3 mL), H_2 (30 bar), $180\,^{\circ}C$, 3 h. Conversion and yield were determined by GC (FID) using an internal standard technique. The carbon balance was more than 95 for all the reactions. b Unknown condensation product of FFalc (according to the GC-MS data).

		Yield ^a (%)						
Entry	Catalyst	Conv. ^a (%)	1,5-PeD (1,2- PeD)	4,5- DHFM	THFalc	CPO (CPL)	2-MeF (2- MeTHF)	Others^b
1	Ru-Sn/γ–Al ₂ O ₃ -C	38	16	0	8	13	0	1
2	Ru - Sn/γ - Al_2O_3 - ZrO_2	93	52	13	0	16	0	12
3	$Ru-Sn/\gamma-Al_2O_3-TiO_2(A)$	81	56	7	5	6	0	7
4	$Ru-Sn/\gamma-Al_2O_3-TiO_2(R)$	43	37	0	4	2	0	0
5	Ru - Sn/γ - Al_2O_3 - ZnO	14	10	0	2	2	0	0
6	Ru - Sn/γ - Al_2O_3 - Nb_2O_5	32	9	1	20	2	0	0

evaluated and the results had been published previously [32]. Therefore, the Ru-Sn/ γ -Al₂O₃-TiO₂(A) (33%) catalyst is set for further optimised reaction conditions (initial H₂ pressure, temperature, and reaction profiles) and discussed subsequently.

3.1.3.2. Effect of initial H₂ pressure

Next, the effect of initial H₂ pressure on FFalc conversion and yield of 1,5-PeD was evaluated using the most effective Ru-Sn/γ-Al₂O₃-TiO₂(A) (33%) catalyst at 180 °C, 10-30 bar H₂ for 3 h and the results are shown in Figure 3. At the initial H₂ pressure of 10 bar, 95% FFalc was converted to 77% 1,5-PeD, 5% THFalc, 9% 4,5-DHFM, and 4%

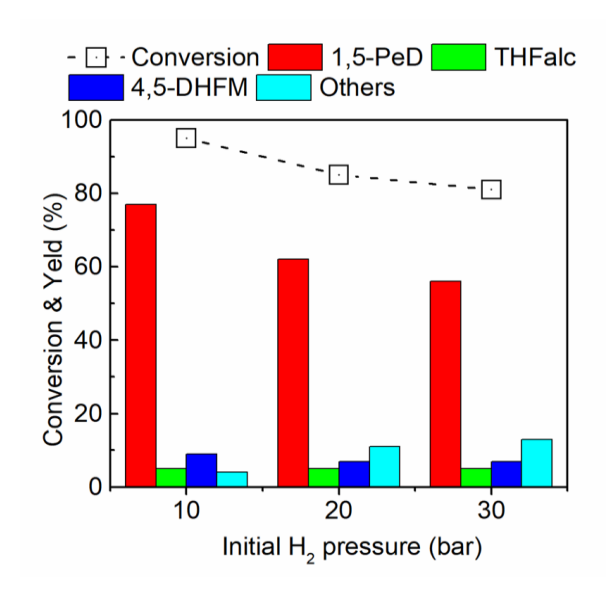


Figure 3. Results of aqueous phase hydrogenolysis of FFalc to 1,5-PeD at different H_2 pressure using Ru-Sn/ γ -Al₂O₃-TiO₂(A) (33%) catalyst. Reaction conditions: Cat. (0.05 g), FFalc (2.0) mmol, H_2 O (3 mL), H_2 (10-30 bar), 180 °C, 3 h.

others. When initial H₂ pressure was increased to 20 bar, the conversion of FFalc slightly decreased to 85% with 1,5-PeD yield of 62%. At this condition, 7% 4,5-DHFM, 5% CPO and 6% others were quantitatively observed, while THFalc remained unchanged. Further increases in initial H₂ pressure to 30 bar, both FFalc conversion and 1,5-PeD yield slightly decreased. It was found that a 81% FFalc was converted to 56% 1,5-PeD, 7% 4,5-DHFM, 5% THFalc, 6% CPO, and 7% others. These results suggest that low initial H₂ pressure (10 bar) of reaction is favorable for the formation of 1,5-PeD. Therefore, this initial H₂ pressure will be applied for evaluating the effect of reaction temperature on FFalc conversion and 1,5-PeD yield using both Ru-Sn/γ-Al₂O₃-TiO₂(A) (33%) and Ru-Sn/ γ -Al₂O₃ catalysts.

3.1.3.3 Effect of reaction temperature

As aforementioned, the optimised initial $\rm H_2$ pressure was 10 bar with highest yield of 1,5-PeD (67%) at 180 °C for 3 h. Next, the evaluation of reaction temperature (c.a. 120-180 °C) over both Ru-Sn/ γ -Al $_2$ O $_3$ and Ru-Sn/ γ -Al $_2$ O $_3$ -TiO $_2$ (33%) catalysts in aqueous phase hydrogenolysis of FFalc to 1,5-PeD was also performed and the results are shown in Figure 4.

In the case of Ru-Sn/ γ -Al₂O₃-TiO₂(A) (33%) catalyst, the conversion of FFalc was 96% to produce 49% 1,5-PeD, 3% THFalc, 38% 4,5-DHFM and 6% others at 120 °C (Figure 4(a). When the reaction temperature was increased to 140 °C, FFalc conversion significantly increased to 92% while 1,5-PeD yield increased to 51% with much high remained 4,5-DHFM (33%). At 160 °C, at similar FFalc conversion (93%), yield of 1,5-PeD increased to 65% while 4,5-DHFM decreased to 18%. Further increase of reaction temperature to 180 °C resulted in high yield of 1,5-PeD (77%)

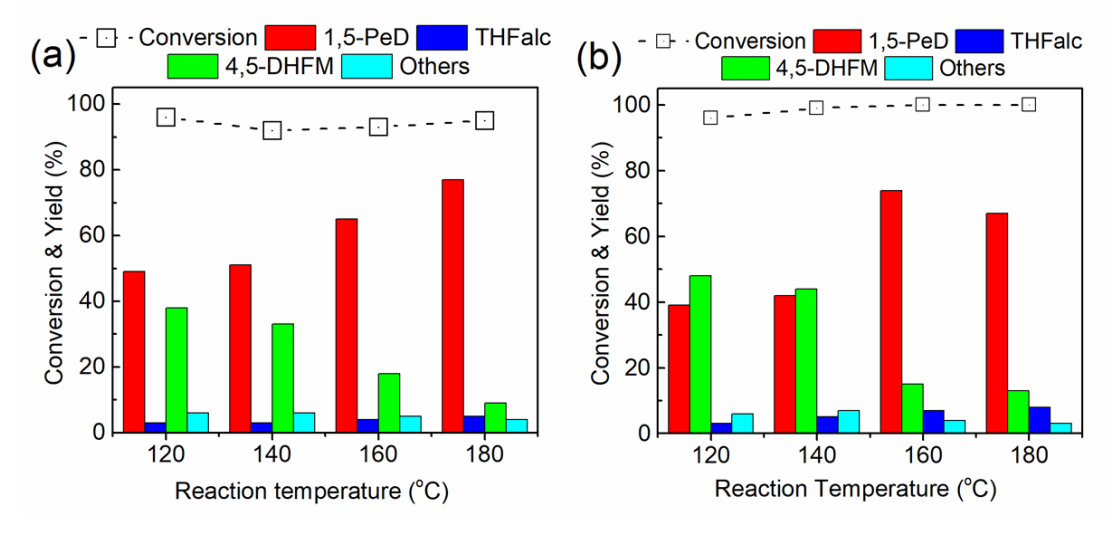


Figure 4. Results of aqueous phase hydrogenolysis of FFalc to 1,5-PeD at different reaction temperatures using (a) Ru-Sn/ γ -Al $_2$ O $_3$ -TiO $_2$ (A) (33%) and (b) Ru-Sn/ γ -Al $_2$ O $_3$ catalysts. Reaction conditions: Cat. (0.05 g), FFalc (2.0) mmol, H $_2$ O (3 mL), H $_2$ (10 bar), 120-180 °C, 3 h.

while the amount of 4,5-DHFM was 9% at 95% conversion of FFalc. It can be observed that the increase in 1,5-PeD yield is symultaneously followed by the decrease in 4,5-DHFM product over both Ru-Sn/y-Al₂O₃ and Ru-Sn/y-Al₂O₃-TiO₂ (33%) catalysts. Interestingly, both Ru-Sn/γ-Al₂O₃ and Ru-Sn/y-Al₂O₃-TiO₂ (33%) catalysts can be catalysed effectively at the initial H₂ pressure of 10 bar at the range temperature of 160-180 °C. In the case of Ru-Sn/ γ -Al₂O₃ catalyst, FFalc conversion increased at the elevated reaction temperature and reached 100% at 160-180 °C (Figure 4(b)). At 120 °C, the amounts of 4,5-DHFM and 1,5-PeD were 48% and 39%, respectively. When the reaction was increased to 140 °C, the amount of 1,5-PeD increased slightly, while 4,5-DHFM decreased oppositely. Further increase in the reaction temperature to 160 °C and 180 °C resulted much high yield of 1,5-PeD, 74% and reaction. 67%, respectively at completed Therefore, further investigation on the attempting to obtain most effective catalyst catalyst (including synthesis procedure, composition, and the recyclability test) with much higher yield of 1,5-PeD under mild reaction conditions is still under going and the results will be published in the subsequent paper.

3.2 Discussion and Structure-activity Relationship

In our recently published work on selective hydrogenolysis of furfural to 1,5-PeD using Ru-Sn/ γ -Al₂O₃ catalyst, the highest yield of 1,5-PeD (94%) was obtained at 180 °C, H₂ 30 bar after 7 h [30]. Herein, a composite of γ -Al₂O₃ was modified with TiO₂(A) (33 wt% TiO₂(A) to γ -Al₂O₃) was employed as the support of Ru-Sn (Ru/Sn molar ratio of 3.0) catalyst. It is found that a comparable yield of 1,5-PeD (80%) was obtained at 99% FFalc conversion at the initial H₂ pressure of 10 bar, 180 °C for 5 h (Table 3, entry 1).

A reusability test of Ru-Sn/ γ -Al₂O₃-TiO₂(A) (33%) catalyst was conducted, and the results are also summarised in Table 4. Around 95% of the spent Ru-Sn/ γ -Al₂O₃-TiO₂(A) (33%) catalyst can be recycled. Results of the reusability test show that FFalc conversion was 97% with 69% yield of 1,5-PeD, 13% 4,5-DHFM, 5% THFalc, 5% CPO, and 5% others (entry 2). The activity Ru-

Sn/y-Al₂O₃-TiO₂(A) (33 wt%) catalyst can be restored the initial after reactivated by H2 at 400 °C for 2 h. After detailed examination, the control of catalytic selectivity, reproducibility, and reusability of this catalyst are still drawback while other supported Ru-based catalysts have poor selectivity. In discussion, we focused on the bimetallic Ru-Sn/y-Al₂O₃-TiO₂(A) (33%) system catalyst in order to find the most suitable support and the highest yield of 1,5-PeD. To get insight into the catalyst structure-activity relationship, the physico-chemical properties (e.g. specific surface area BET (SBET), porosity, pore volume, surface acidity, metal dispersion, and average Ru-Sn nanoparticles sizes), and XRD analysis of three types supported Ru-Sn catalysts were examined.

Figure 5 shows the N₂ adsorption-desorption profiles of three types supported Ru-Sn catalysts. The N₂ adsorption-desorption profiles confirmed the major pore structure of samples containing micropores and mesopore. The portion of mesopores dramatically increased in $Sn/\gamma - Al_2O_3 - TiO_2(A)$ (33%)as depicted volumetric adsorption of N₂ (STP) (cm³/g), average pore width profiles, and pore volume (cm³/g). It is found that the pore width and pore volume of this sample were 22.1 nm and 0.54 cm³/g, respectively. These properties may affect the interaction between catalyst surface and substrate (FFalc) during the reaction, consequently, the product distribution over this catalyst differs from the other catalysts. However, detailed more investigation on the role of pore structure, pore width, and pore volume in the improvement of 1,5-PeD yield from FFalc is needed for confirmation of the suggestion. Moreover, the specific surface area BET (S_{BET}) of Ru-Sn/TiO₂(A), Ru-Sn/y-Al₂O₃, and Ru-Sn/ γ -Al₂O₃-TiO₂(A) (33%) were 63.4 m²/g, 132 m²/g, 128 m²/g, respectively while the pore volume was $0.02 \text{ cm}^3/\text{g}$, $0.09 \text{ cm}^3/\text{g}$, $0.54 \text{ cm}^3/\text{g}$, respectively (Table 4).

Figure 6 shows the XRD patterns of three types supported Ru-Sn on different supports after reduction with $\rm H_2$ at 400 °C for 2 h. The pristine structures of $\rm TiO_2$ anatase are clearly observed at $2\theta=25.3^{\circ},\ 37.8^{\circ},\ 48.0^{\circ},\ 54.0^{\circ},\ 55.1^{\circ},\ 62.7^{\circ},\ 68.8^{\circ},\ 70.2^{\circ},\ and\ 75.1^{\circ},\ (JCPDS\ No.\ 21-1276)$ with average crystallite sizes of $\rm TiO_2\ (101)\ (2\theta=25.3^{\circ})$ of 44.2 nm (Figure 6(a)). The diffraction peaks of

Table 3. Results of aqueous phase hydrogenolysis of furfuryl alcohol using Ru-Sn/ γ -Al₂O₃-TiO₂(A) (33%) catalyst.

	Descrion	Conv. ^a (%)	Yield ^a (%)						
Entry	Reaction time (h)		1,5-PeD (1,2-PeD)	4,5- DHFM	THFalc	CPO (CPL)	2-MeF (2- MeTHF)	Others^b	
1	5	99	80	7	7	0	0	5	
2^c	3	97	69	13	5	5	0	5	

TiO₂ anatase become broadened after mixed with γ -Al₂O₃ and the average crystallite sizes of TiO₂ (101) (20 = 25.3°) of 14.7 nm (Figure 6 (c)). In the case of Ru-Sn/ γ -Al₂O₃ sample, typical diffraction peak at 20 = 67° is observed and the peak become broadened after mixed with TiO₂(A) (Figure 6(b)).

The H₂-TPR profiles of Ru-Sn/γ-Al₂O₃ and Ru-Sn/γ-Al₂O₃-TiO₂(A) (33%) catalysts are shown in Figure 7, and the data are also summarised in Table 5. The hydrogen-temperature programmed reduction (H₂-TPR) of catalysts help to identify the surface species during the hydrogen reduction process. A high intensity of reduction peak at 58 °C dan two distinctive reduction peaks of RuO2 to Ru⁰ were observed at 92 °C and 120 °C, suggesting the existence of RuO2 interacting with TiO2 and g- Al_2O_3 supports, respectively, during preparation of catalyst for both Ru-Sn/y-Al₂O₃ and Ru-Sn/γ-Al₂O₃-TiO₂(A) (33 wt%) catalysts (Figure 7(a & b). Both catalysts also show a broad reduction peak at 302 °C which can be assigned as the typical reduction of RuO2-SnO2 to form Ru3Sn7 alloy which has strong interaction with the support. In the Ru-Sn/ γ -Al₂O₃-TiO₂(A) (33%) catalyst, exhibited much higher intensity than that of Ru-Sn/y-Al₂O₃, indicating much greater hydrogen was consumed to transform RuO₂-SnO₂ to Ru₃Sn₇ alloy phase with high existence of RuO₂-SnO₂ species and intimate interactions between

Table 4. Porosity properties (specific surface area BET (S_{BET}), pore width, and pore volume) of synthesised supported bimetallic Ru-Sn catalysts.

Entry	Catalyst	$S_{ m BET}^a \ ({ m m}^2.~{ m g}^{ ext{-}1})$	Pore width ^b (nm)	Vp ^b (cm ³ /g)
1	Ru-Sn/TiO ₂ (A)	63	2.7	0.02
2	Ru - Sn/γ - Al_2O_3	132	1.7	0.09
3	Ru-Sn/γ–Al ₂ O ₃ -	128	22.1	0.54
	$TiO_2(A)$ (33%)			

them [40]. However, the XRD patterns of that sample did not show the presence of the remaining SnO₂ species (Figure 6). It is found that the H₂ uptakes of Ru-Sn/y-Al₂O₃ and Ru-Sn/y-Al₂O₃-TiO₂(A) (33%) catalysts were 5.34 mmol.g-1 and 3.11 mmol.g⁻¹ respectively (Table 5, entries 2-3). These results indicate that the active sites of Ru may be partially covered by the presence of much higher Sn co-loaded which can hinder the chemisorption of hydrogen as indicated by decreasing the H2 uptake. The dispersion and particles sizes of Ru were also estimated from the H₂ uptake data using the proposed equation of Suib et al. with an assumption that the surface area occupied by an exposed surface of Ru(001) [35]. It is found that the dispersion (D) was 21% and 12.5% with Ru particle sizes of 4.2 nm and 7.2 nm (Table 5, entries 2 and 3).

To assess the role of surface acidity of the catalysts, the NH₃-TPD measurement for Ru-Sn/TiO₂(A), Ru-Sn/ γ -Al₂O₃, and Ru-Sn/ γ -Al₂O₃-TiO₂(A) (33%) samples were conducted, and the results are shown in Figure 8. The NH₃-TPD

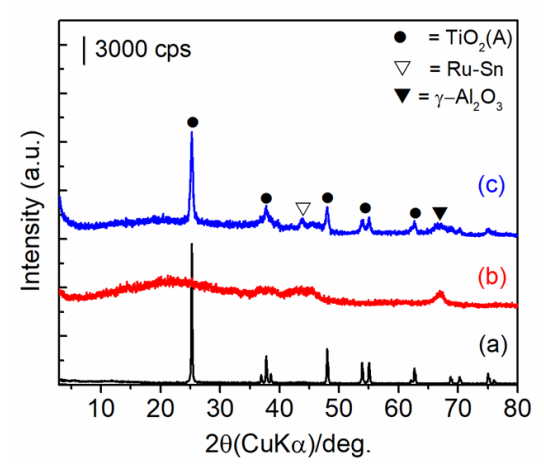


Figure 6. XRD patterns of (a) Ru-Sn/TiO₂(A), (b) Ru-Sn/g-Al₂O₃, and (c) Ru-Sn/ γ -Al₂O₃-TiO₂(A).

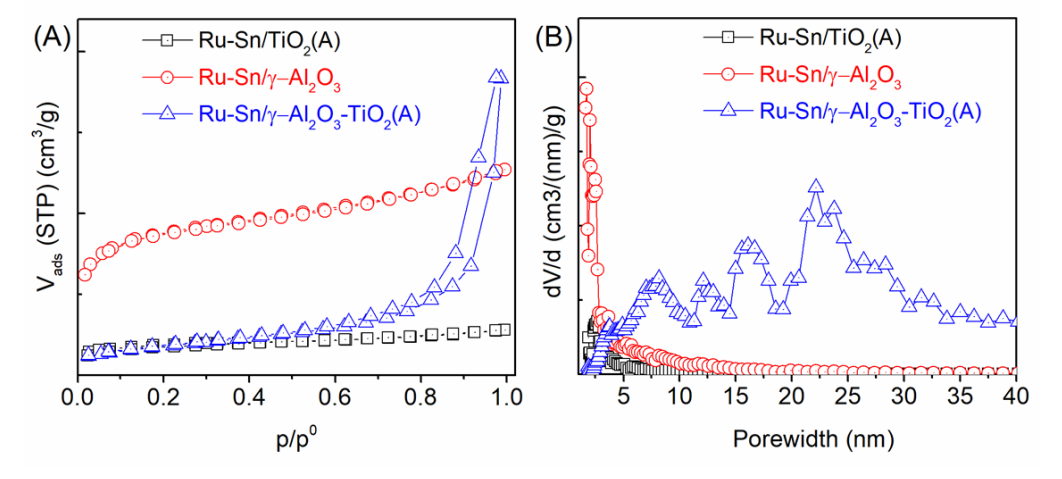


Figure 5. (A) N₂-adsorption/desorption profiles and (B) pore sizes distribution (nm) for three types supported bimetallic Ru-Sn catalysts.

profiles were formally divided into three desorption temperature regions to denote three types of acid sites [41,42] (1) weak acid sites, ranging from 100 to 200 °C, (2) moderate acid sites, ranging from 200 to 550 °C, and (3) strong acid sites, ranging from >550 °C (Figure 8). Ru-Sn/TiO₂(A) has a desorption peak at 177.2 °C (weak acid), and three desorption peaks (strong acid) at 579.5 °C, 610.4 and a small shoulder peak at 680.5 °C with total acidity of 124 mmol NH₃ per gram (Figure 8(a), which may affect the product selectivity. Though Ru-Sn/y-Al₂O₃ has much higher total acidity (1108 µmol NH3 per gram) than that other catalysts, the portion of moderate acid sites is proportional to the strong acid sites (Figure 8(b)). As a result, the selectivity toward 1,5-PeD higher than that obtained 1,5-PeD from Ru-Sn/TiO₂(A) catalyst (Table 1, entry 4). Indeed, Ru-Sn/ γ -Al₂O₃-TiO₂(A) (33%) catalyst has total acidity of 718 µmol NH3 per gram comprised of higher weak acid site portion (Figure 8(c)) and exhibited comparable yield of 1,5-PeD to the unmodified Ru-Sn/ γ -Al₂O₃ catalysts (Table 2,

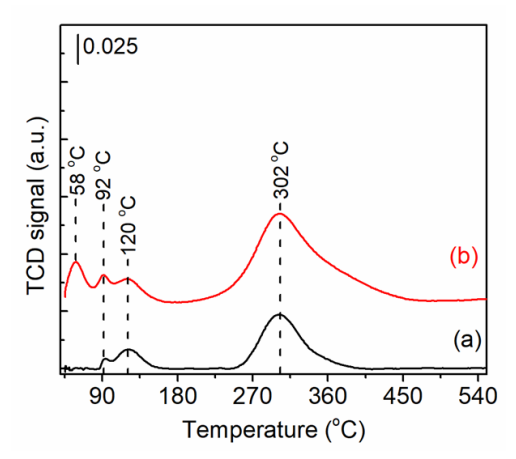


Figure 7. H₂-TPR profiles of (a) Ru-Sn/ γ -Al₂O₃ and (b) Ru-Sn/ γ -Al₂O₃-TiO₂(A) (33%) catalysts.

Table 5. Physico-chemical properties (H₂-uptake, metal dispersion, particle diameter, and acidity) of synthesised supported bimetallic Ru-Sn catalysts. ^aThe H₂ uptake was derived from H₂-TPR data. ^bMetal dispersion (%). ^cRu particle sizes (nm). ^dAverage crystallite sizes of TiO₂ anatase (2θ =25.3°) using Scherrer's equation. ^cAcidity was derived from NH₃-TPD spectra. n.d. = not determined.

Entry	Catalyst	$ m H_2~uptake^a \ (mmol.g^{-1})$	D^b (%)	$d_{\mathrm{VA}^c} \ \mathrm{(nm)}$	${ m TiO}_2{}^d \ ({ m nm})$	Acidity ^e (μmol NH ₃ .g ⁻¹)
1	Ru-Sn/TiO ₂ (A)	n.d	n.d.	n.d.	44.2	124
2	Ru-Sn/γ–Al ₂ O ₃	5.34	21.4	4.2	n.d	1108
3	Ru-Sn/ ν -Al $_{2}O_{3}$ -Ti $O_{2}(A)$ (33%)	3.11	12.5	7.2	14.7	718

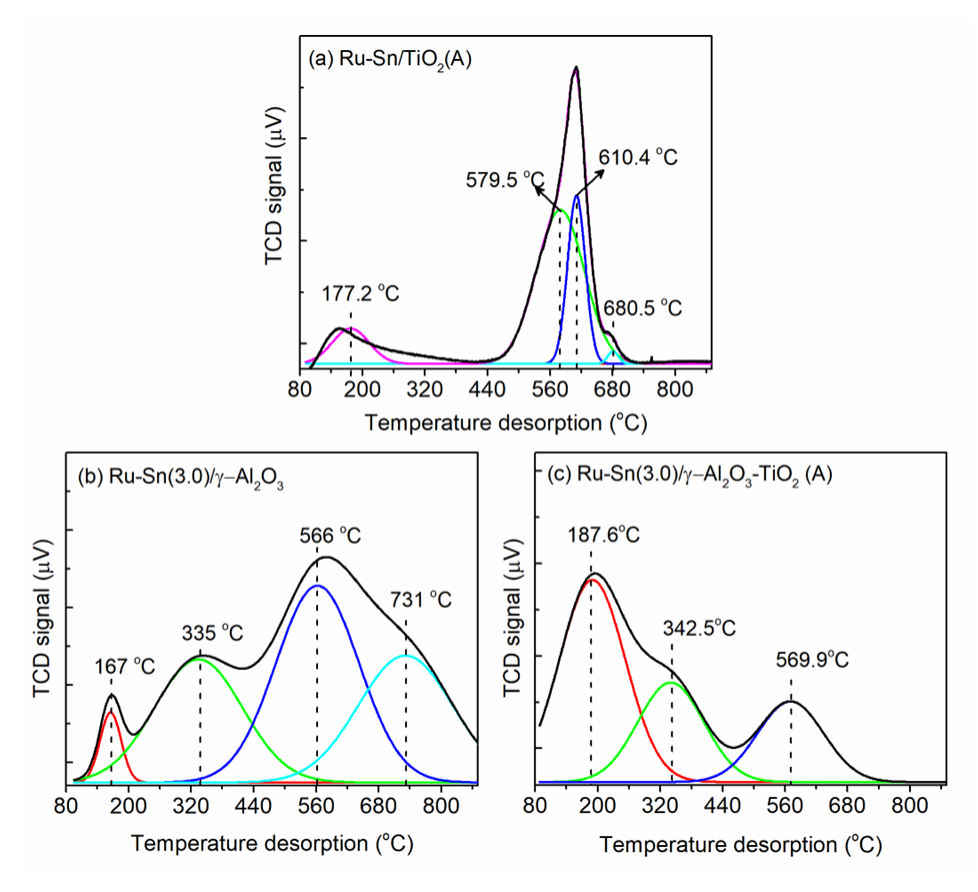


Figure 8. NH₃-TPD profiles of (a) Ru-Sn/TiO₂(A), (b) Ru-Sn/ γ -Al₂O₃, and (c) Ru-Sn/ γ -Al₂O₃-TiO₂(A) (33%) catalysts after reduction with H₂ at 400 °C for 2 h.

entry 3). The recyclability and reusability test of Ru-Sn/ γ -Al₂O₃-TiO₂(A) (33%) catalyst exhibited that the composited γ -Al₂O₃-TiO₂ is more stable than that of unmodified Ru-Sn/TiO₂(A) and Ru-Sn/ γ -Al₂O₃ catalysts. Therefore, it can be concluded that the high selectivity of 1,5-PeD from aqueous phase hydrogenolysis of FFalc over bimetallic supported Ru-Sn catalyst may be affected by controlling the acidity of support. Further investigation into the role distinguished acid site, Bronsted or Lewis acid sites in the catalyst system are necessary.

4. Conclusions

Investigation on the screening support of bimetallic ruthenium-tin catalysts for selective aqueous phase hydrogenolysis of furfuryl alcohol into 1,5-PeD at 180 °C, initial H₂ 10-30 bar for 3-5 h were described systematically. The TiO₂(A), γ-Al₂O₃, and ZrO₂ supported Ru-Sn catalysts exhibited a higher yield of 1,5-PeD (55-69%) than that other catalysts at 180 °C, H₂ 10-30 bar for 3-5 h. However, those supported catalysts showed poor recyclability after the first reaction run, and therefore, further examination on γ–Al₂O₃ by combination with various metal oxides (e.g., ZrO₂, TiO₂(A), TiO₂(R), ZnO, Nb₂O₅, and C) to form γ-Al₂O₃-metal oxide composites support was performed. The Ru-Sn supported on γ-Al₂O₃metal oxide composites (metal oxides:) afforded similar FFalc conversion and yield of 1,5-PeD than that of unmodified γ-Al₂O₃ at 180 °C, H₂ 30 bar for 3. Among them, the Ru-Sn/γ-Al₂O₃-TiO₂(A) (33%) catalyst could afford the highest yield of 1,5-PeD (80%) at 99% conversion FFalc at 180 °C, H₂ 10 bar for 5 h. This catalyst can be recycled (95% from the initial) after the second reaction run and the activity can be restored to initial after reactivation with H2 at 400 °C for 2 h and passivated with N_2 for 20 min. Results of catalyst characterisation confirm the presence bimetallic Ru-Sn on the support of γ-Al₂O₃-TiO₂ (A). The high selectivity of 1,5-PeD from aqueous phase hydrogenolysis of FFalc over bimetallic supported Ru-Sn catalyst may be affected by controlling the acidity of support. Further investigation into the distinguishing acid sites, Lewis or Brønsted acid sites in the catalyst system and its role during the catalytic reaction are necessary. Though the selectivity of Ru- $Sn/\gamma-Al_2O_3-TiO_2(A)$ (33%) catalyst toward 1,5-PeD is similar to the unmodified Ru-Sn/y-Al₂O₃, the degree of recyclability significantly enhanced after the modification.

Acknowledgement

The authors acknowledge The Indonesian Endowment Funds for Education (LPDP) through BRIN-RIIM2 scheme (contract number of 79/IV/KS/11/2022), DRPTM-Kemendiktisaintek

through Regular Fundamental scheme (contract number of 056/E5/PG.02.00.PL/2024), and LPPM-ULM through Internal Fundamental scheme (contract number of 1374.95/UN8.2/PG/2024) for financial support. We also acknowledge the facilities, scientific and technical support from Advanced Chemical Characterization Laboratory, National Research, and Innovation Agency through E- Layanan Sains - BRIN.

CRediT Author Statement

Author Contributions: Atina Sabila Azzahra, Ridhoni, Ikhsan Mustari, Anggita Nurfitriani, Thea Seventina Desiani Bodoi: Formal Analysis, Investigation, Experiment, Writing-Original Draft. Rodiansono, Rahmat Eko Saniava: Conceptualization, Methodology, Writing-Review & Editing, Supervision. Eka Suarso, Pathur Razi Ansyah: Formal Analysis and Advanced Characterisation. All authors have read and agreed to the published version of the manuscript.

References

- [1] Gérardy, R., Debecker, D.P., Estager, J., Luis, P., Monbaliu, J.C.M. (2020). Continuous Flow Upgrading of Selected C2-C6 Platform Chemicals Derived from Biomass. *Chemical Reviews*, 120(15), 7219–7347. DOI: 10.1021/acs.chemrev.9b00846.
- [2] Tomishige, K., Nakagawa, Y., Tamura, M. (2017). Selective hydrogenolysis and hydrogenation using metal catalysts directly modified with metal oxide species. Green Chemistry, 19(13), 2876–2924. DOI: 10.1039/c7gc00620a.
- [3] Xu, C., Paone, E., Rodríguez-Padrón, D., Luque, R., Mauriello, F. (2020). Recent catalytic routes for the preparation and the upgrading of biomass derived furfural and 5-hydroxymethylfurfural. *Chemical Society Reviews*, 49(13), 4273–4306. DOI: 10.1039/d0cs00041h.
- [4] Sun, X., Wen, B., Wang, F., Zhang, W., Zhao, K., Liu, X. (2024). Research advances on the catalytic conversion of biomass-derived furfural into pentanediols. *Catalysis Communications*, 187, 106864. DOI: 10.1016/j.catcom.2024.106864.
- [5] Tomishige, K., Honda, M., Sugimoto, H., Liu, L., Yabushita, M., Nakagawa, Y. (2024). Recent progress on catalyst development for ringopening C-O hydrogenolysis of cyclic ethers in the production of biomass-derived chemicals. *Carbon Neutrality*, 3(1), 17. DOI: 10.1007/s43979-024-00090-y.
- [6] Xu, W., Wang, H., Liu, X., Ren, J., Wang, Y., Lu, G. (2011). Direct catalytic conversion of furfural to 1,5-pentanediol by hydrogenolysis of the furan ring under mild conditions over Pt/Co2AlO4 catalyst. *Chemical Communications*, 47(13), 3924–3926. DOI: 10.1039/c0cc05775d.

- [7] Tong, T., Xia, Q., Liu, X., Wang, Y. (2017). Direct hydrogenolysis of biomass-derived furans over Pt/CeO2 catalyst with high activity and stability. Catalysis Communications, 101, 129–133. DOI: 10.1016/j.catcom.2017.08.005.
- [8] Tong, T., Liu, X., Guo, Y., Norouzi Banis, M., Hu, Y., Wang, Y. (2018). The critical role of CeO2 crystal-plane in controlling Pt chemical states on the hydrogenolysis of furfuryl alcohol to 1,2pentanediol. *Journal of Catalysis*, 365, 420–428. DOI: 10.1016/j.jcat.2018.07.023.
- [9] Liu, S., Amada, Y., Tamura, M., Nakagawa, Y., Tomishige, K. (2014). One-pot selective conversion of furfural into 1,5-pentanediol over a Pd-added Ir–ReOx/SiO2 bifunctional catalyst. Green Chemistry, 16(2), 617. DOI: 10.1039/c3gc41335g.
- [10] Koso, S., Furikado, I., Shimao, A., Miyazawa, T., Kunimori, K., Tomishige, K. (2009). Chemoselective hydrogenolysis of tetrahydrofurfuryl alcohol to 1,5-pentanediol. *Chemical Communications*, (15), 2035–2037. DOI: 10.1039/b822942b.
- [11] Sun, D., Sato, S., Ueda, W., Primo, A., Garcia, H., Corma, A. (2016). Production of C4 and C5 alcohols from biomass-derived materials. Green Chemistry, 18(9), 2579–2597. DOI: 10.1039/c6gc00377j.
- [12] Li, X., Jia, P., Wang, T. (2016). Furfural: A Promising Platform Compound for Sustainable Production of C4 and C5 Chemicals. ACS Catalysis, 6(11), 7621–7640. DOI: 10.1021/acscatal.6b01838.
- [13] Wijaya, H.W., Hara, T., Ichikuni, N., Shimazu, S. (2018). Hydrogenolysis of tetrahydrofurfuryl alcohol to 1,5-pentanediol over a nickel-yttrium oxide catalyst containing ruthenium. *Chemistry Letters*, 47(1), 103–106. DOI: 10.1246/cl.170920.
- [14] Tan, J., Su, Y., Hai, X., Huang, L., Cui, J., Zhu, Y., Wang, Y., Zhao, Y. (2022). Conversion of furfuryl alcohol to 1,5-pentanediol over CuCoAl nanocatalyst: The synergetic catalysis between Cu, CoOx and the basicity of metal oxides. *Molecular Catalysis*, 526, 112391. DOI: 10.1016/j.mcat.2022.112391.
- [15] Liu, H., Huang, Z., Zhao, F., Cui, F., Li, X., Xia, C., Chen, J. (2016). Efficient hydrogenolysis of biomass-derived furfuryl alcohol to 1,2- and 1,5-pentanediols over a non-precious Cu-Mg3AlO4.5 bifunctional catalyst. Catalysis Science and Technology, 6(3), 668–671. DOI: 10.1039/c5cy01442e.
- [16] Barranca, A., Gandarias, I., Arias, P.L., Agirrezabal-Telleria, I. (2023). One-Pot Production of 1,5-Pentanediol from Furfural Through Tailored Hydrotalcite-Based Catalysts. Catalysis Letters, 153(7), 2018–2025. DOI: 10.1007/s10562-022-04144-7.
- [17] Fu, X., Ren, X., Shen, J., Jiang, Y., Wang, Y., Orooji, Y., Xu, W., Liang, J. (2021). Synergistic catalytic hydrogenation of furfural to 1,2-pentanediol and 1,5-pentanediol with LDO derived from CuMgAl hydrotalcite. *Molecular Catalysis*, 499(July 2020), 111298. DOI: 10.1016/j.mcat.2020.111298.

- [18] Shen, Q., Li, Y., Wang, F., Zhang, X., Zhang, Z., Zhang, Z., Yang, Y., Bing, C., Fan, X., Zhang, J., He, X. (2024). Controlled targeted conversion of furfural to 1,5-pentanediol or 2-methylfuran over Ni/CoAlOx catalyst. *Molecular Catalysis*, 556, 113919. DOI: 10.1016/j.mcat.2024.113919.
- [19] Peng, J., Zhang, D., Wu, Y., Wang, H., Tian, X., Ding, M. (2023). Selectivity control of furfuryl alcohol upgrading to 1,5-pentanediol over hydrotalcite-derived Ni-Co-Al catalyst. Fuel, 332, 126261. DOI: 10.1016/j.fuel.2022.126261.
- [20] Liu, D., Fu, J., Wang, J., Zhu, X., Xu, J., Zhao, Y., Huang, J. (2024). Interfacial synergy within bimetallic oxide promotes selective hydrogenolysis of furfuryl alcohol to 1,5-pentanediol. *Applied Surface Science*, 642, 158571. DOI: 10.1016/j.apsusc.2023.158571.
- [21] Upare, P.P., Kim, Y., Oh, K.R., Han, S.J., Kim, S.K., Hong, D.Y., Lee, M., Manjunathan, P., Hwang, D.W., Hwang, Y.K. (2021). A Bimetallic Ru3Sn7Nanoalloy on ZnO Catalyst for Selective Conversion of Biomass-Derived Furfural into 1,2-Pentanediol. ACS Sustainable Chemistry and Engineering, 9(51), 17242–17253. DOI: 10.1021/acssuschemeng.1c05322.
- [22] Nimbalkar, A.S., Oh, K.-R., Hong, D.-Y., Park, B.G., Lee, M., Hwang, D.W., Awad, A., Upare, P.P., Han, S.J., Hwang, Y.K. (2024). Continuous production of 1,2-pentanediol from furfuryl alcohol over highly stable bimetallic Ni–Sn alloy catalysts. *Green Chemistry*, 26(22), 11164–11176. DOI: 10.1039/D4GC02757D.
- [23] Brentzel, Z.J., Barnett, K.J., Huang, K., Maravelias, C.T., Dumesic, J.A., Huber, G.W. (2017). Chemicals from Biomass: Combining Ring-Opening Tautomerization and Hydrogenation Reactions to Produce 1,5-Pentanediol from Furfural. ChemSusChem, 10(7), 1351–1355. DOI: 10.1002/cssc.201700178.
- [24] Rodiansono, R., Hara, T., Ichikuni, N., Shimazu, S. (2012). A novel preparation method of Ni-Sn alloy catalysts supported on aluminium hydroxide: Application to chemoselective hydrogenation of unsaturated carbonyl compounds. *Chemistry Letters*, 41(8), 769–771. DOI: 10.1246/cl.2012.769.
- [25] Rodiansono, R., Hara, T., Ichikuni, N., Shimazu, S. (2014). Development of nanoporous Ni-Sn alloy and application for chemoselective hydrogenation of furfural to furfuryl alcohol. Bulletin of Chemical Reaction Engineering & Catalysis, 9(1), 53–59. DOI: 10.9767/bcrec.9.1.5529.53-59.
- [26] Rodiansono, R., Astuti, M.D., Mujiyanti, D.R., Santoso, U.T., Shimazu, S. (2018). Novel preparation method of bimetallic Ni-In alloy catalysts supported on amorphous alumina for the highly selective hydrogenation of furfural. *Molecular Catalysis*, 445, 52–60. DOI: 10.1016/j.mcat.2017.11.004.

- [27] Rodiansono, R., Astuti, M.D., Husain, S., Nugroho, A., Sutomo, S. (2019). Selective conversion of 2-methylfuran to 1,4-pentanediol catalyzed by bimetallic Ni-Sn alloy. Bulletin of Chemical Reaction Engineering & Catalysis, 14(3), 529–541. DOI: 10.9767/bcrec.14.3.4347.529-541.
- [28] Rodiansono, R., Azzahra, A.S., Ansyah, P.R., Husain, S., Shimazu, S. (2023). Rational design for the fabrication of bulk Ni 3 Sn 2 alloy catalysts for the synthesis of 1,4-pentanediol from biomass-derived furfural without acidic co-catalysts. *RSC Advances*, 13(31), 21171–21181. DOI: 10.1039/D3RA03642A.
- [29] Rodiansono, R., Astuti, M.D., Mustikasari, K., Husain, S., Ansyah, P.R., Hara, T., Shimazu, S. (2022). Unravelling the one-pot conversion of biomass-derived furfural and levulinic acid to 1,4-pentanediol catalysed by supported RANEY® Ni-Sn alloy catalysts. RSC Advances, 12(1), 241–250. DOI: 10.1039/d1ra06135f.
- [30] Rodiansono, R., Azzahra, A.S., Santoso, U.T., Mikrianto, E., Suarso, E., Sembiring, K.C., Adilina, I.B., Sunnardianto, G.K., Afandi, A. (2025). Highly efficient and selective aqueous phase hydrogenolysis of furfural to 1,5-pentanediol using bimetallic Ru–SnO_x/γ-Al ₂ O ₃ catalysts. *Catalysis Science & Technology*, 15(3), 808–821. DOI: 10.1039/D4CY01138D.
- [31] Azzahra, A.S., Annisa, N., Rodiansono, R., Trisno Santoso, U., Eko Sanjaya, R., Suarsa, E. (2025). Effect of Charcoal-Doping on The Yield of 1,5-Pentanediol and Reusability in Ru-Sn/g-Al2O3-Charcoal Catalysts. In: 1st ICWSDGs2024. AIP Conference Proceedings, pp. xxx-xxx.
- [32] Thea, S.D.B., Azzahra, A.S., Ridho Ansyari, M., Mikrianto, E., Rodiansono, R., Eko Sanjaya, R., Razi Ansyah, P. (2025). Selective Conversion of Furfuryl Alcohol to 1,5-Pentanediol Over Ru-Sn/y-Al2O3-TiO2: Effect of Calcination Temperature of y-Al2O3-TiO2. In: 1st ICWDGs2024. AIP Conference Proceedings, p. xxx.
- [33] Azzahra, A.S., Dewi, H.P., Mikrianto, E., Sembiring, K.C., Sunnardianto, G.K., Nata, I.F., Rodiansono, R., Jayanudin, J. (2023). Bimetallic Ru-Sn as Effective Catalysts for the Selective Hydrogenation of Biogenic Platform Chemicals at Room Temperature. Bulletin of Chemical Reaction Engineering & Catalysis, 18(4), 700–712. DOI: 10.9767/bcrec.20067.
- [34] Lowell, S., Shields, J.E., Thomas, M.A., Thommes, M. (2004). Characterization of Porous Solids and Powders: Surface Area, Pore Size and Density. Dordrecht: Springer Netherlands.

- [35] Shen, X., Garces, L.-J., Ding, Y., Laubernds, K., Zerger, R.P., Aindow, M., Neth, E.J., Suib, S.L. (2008). Behavior of H2 chemisorption on Ru/TiO2 surface and its application in evaluation of Ru particle sizes compared with TEM and XRD analyses. Applied Catalysis A: General, 335(2), 187–195. DOI: 10.1016/j.apcata.2007.11.017.
- [36] Kellner, C., Bell, A.T. (1982). Effects of dispersion on the activity and selectivity of alumina-supported ruthenium catalysts for carbon monoxide hydrogenation. *Journal of Catalysis*, 75(2), 251–261. DOI: 10.1016/0021-9517(82)90207-X.
- [37] Khaja Masthan, S., Rao, R., Chary, V.R., Rao, V., Rao, K. (1994). Influence of metal loading and temperature on hydrogen chemisorption and hydrogenation activity of Ru/gamma-Al2O3 catalysts. *Indian Journal of Chemistry*, 33, 26– 32.
- [38] Gueye, I., Kim, J., Kumara, L.S.R., Yang, A., Seo, O., Chen, Y., Song, C., Hiroi, S., Kusada, K., Kobayashi, H., Kitagawa, H., Sakata, O. (2019). Investigation of selective chemisorption of fcc and hcp Ru nanoparticles using X-ray photoelectron spectroscopy analysis. *Journal of Catalysis*, 380, 247–253. DOI: 10.1016/j.jcat.2019.10.004.
- [39] Li, X., Deng, Q. (2023). Review on Metal—Acid Tandem Catalysis for Hydrogenative Rearrangement of Furfurals to C5 Cyclic Compounds. *Transactions of Tianjin University*, 29(5), 347–359. DOI: 10.1007/s12209-023-00367-w.
- [40] Luo, Z., Bing, Q., Kong, J., Liu, J.Y., Zhao, C. (2018). Mechanism of supported Ru3Sn7 nanocluster-catalyzed selective hydrogenation of coconut oil to fatty alcohols. *Catalysis Science and Technology*, 8(5), 1322–1332. DOI: 10.1039/c8cy00037a.
- [41] Wang, J., Chernavskii, P.A., Wang, Y., Khodakov, A.Y. (2013). Influence of the support and promotion on the structure and catalytic performance of copper-cobalt catalysts for carbon monoxide hydrogenation. *Fuel*, 103, 1111–1122. DOI: 10.1016/j.fuel.2012.07.055.
- [42] Khandan, N., Kazemeini, M., Aghaziarati, M. (2008). Determining an optimum catalyst for liquid-phase dehydration of methanol to dimethyl ether. *Applied Catalysis A: General*, 349(1–2), 6–12. DOI: 10.1016/j.apcata.2008.07.029.